

This article was downloaded by: [University of Haifa Library]

On: 13 August 2012, At: 20:40

Publisher: Taylor & Francis

Informa Ltd Registered in England and Wales Registered Number: 1072954 Registered office: Mortimer House, 37-41 Mortimer Street, London W1T 3JH, UK



## Molecular Crystals and Liquid Crystals

Publication details, including instructions for authors and subscription information:

<http://www.tandfonline.com/loi/gmcl20>

### Extension of Phase Modulation Ellipsometry to Measure Refractive Indices of Liquid Crystals

E. Batella<sup>a</sup>, A. D'ALESSANDRO<sup>a</sup> & M. Warenghem<sup>b</sup>

<sup>a</sup> Dipartimento di Ingegneria Elettronica, Università degli Studi di Roma "La Sapienza", Istituto Nazionale per la Fisica della Materia, Via Eudossiana, 18, Roma, 00184

<sup>b</sup> Laboratoire de Physico-Chimie des Interfaces et Applications (EA 2463), Université d'Artois, Rue Jean Souvraz; SP 18, LENS Cedex, 62307

Version of record first published: 29 Oct 2010

To cite this article: E. Batella, A. D'ALESSANDRO & M. Warenghem (2002): Extension of Phase Modulation Ellipsometry to Measure Refractive Indices of Liquid Crystals, *Molecular Crystals and Liquid Crystals*, 372:1, 275-289

To link to this article: <http://dx.doi.org/10.1080/10587250127574>

PLEASE SCROLL DOWN FOR ARTICLE

Full terms and conditions of use: <http://www.tandfonline.com/page/terms-and-conditions>

This article may be used for research, teaching, and private study purposes. Any substantial or systematic reproduction, redistribution, reselling, loan, sub-licensing, systematic supply, or distribution in any form to anyone is expressly forbidden.

The publisher does not give any warranty express or implied or make any representation that the contents will be complete or accurate or up to date. The accuracy of any instructions, formulae, and drug doses should be independently verified with primary sources. The publisher shall not be liable for any loss, actions, claims, proceedings, demand, or costs or damages whatsoever or howsoever caused arising directly or indirectly in connection with or arising out of the use of this material.

## Extension of Phase Modulation Ellipsometry to Measure Refractive Indices of Liquid Crystals

E. BATELLA<sup>a</sup>, A. d'ALESSANDRO<sup>a</sup> and M. WARENGHEM<sup>b</sup>

<sup>a</sup>*Dipartimento di Ingegneria Elettronica, Università degli Studi di Roma "La Sapienza", Istituto Nazionale per la Fisica della Materia, via Eudossiana, 18 - 00184 Roma and*

<sup>b</sup>*Laboratoire de Physico-Chimie des Interfaces et Applications (EA 2463), Université d'Artois, Rue Jean Souvraz; SP 18 62307 LENS Cedex*

**Abstract** We present an extension of phase modulation ellipsometry to measure refractive indices in the visible and near infrared spectrum of multilayer and anisotropic structures, in particular liquid crystal cells, with arbitrary orientation of optical axis. An original software code was derived to process ellipsometer measurements, based on Jones formalism to express sinusoidal components of detected optical intensity reflected by a sample for different angles of the polariser and analyser respect to the sample orientation. In this way it is possible to obtain independent equations whose unknowns are the reflection matrix coefficients. Since it is possible only to obtain values of detected intensity and reflection coefficients given the refractive indices of the sample by using Berreman formalism, an algorithm has been developed to search best refractive index values which fit intensity measurements at each wavelength. Dispersion curves of refractive indices of 5CB have been obtained with accuracy of about 1%.

**Keywords** refractive indices; nematic liquid crystals; ellipsometry.

## INTRODUCTION

Interest in liquid crystals as promising materials to fabricate photonic devices for telecommunications has been greatly increasing lately. Design and realisation of liquid crystal based photonic devices require accurate information about values of refractive indices, not only birefringence as for flat panel display applications, in the spectral region of 1.3  $\mu\text{m}$  and 1.55  $\mu\text{m}$ , corresponding to optical fibre minimum transmission losses. Measurement of refractive indices of liquid crystals is more difficult than measurements of refractive index of inorganic crystals because it is necessary to confine them in thin cells, where other films, such as alignment layers and electrodes, are present. Since the early works up of M. Brunet [1] most of the index measurements have been performed using refractometry [2], diffractometry [3] or half leaky modes analysis [4]. In some cases these methods allow to obtain some information on the cell structure as well [5][6]. Ellipsometry has been used mainly to determine cells structures [7].

Ellipsometry is a simple, accurate and fast technique to obtain both real and imaginary part of refractive indices through measurements of complex reflection coefficients. Ellipsometry fully automated and allowing a comprehensive set of measurements in polarimetry (Stokes parameters) are commercially available. In particular rotating analyzer ellipsometry (RAE) has been successfully employed to measure indices of anisotropic samples and also refractive indices of liquid crystals [8][9][10]. Moreover phase modulated ellipsometry (PME) is a recently developed technique, based on light modulation by a photo-elastic modulator, which improves RAE performance in terms of measurement speed and accuracy by reducing mechanical vibrations.

In this paper we present a new method of processing measurements provided by a phase modulated ellipsometer for multilayered anisotropic structures embedded between two isotropic semi-infinite media called ambient and substrate respectively. Our method, based on a fitting algorithm, allows to evaluate the optical main tensor  $\underline{\underline{\epsilon}}$  and its spatial orientation in a wide spectrum of wavelengths, in particular visible and near infrared spectrum. The possibility to include optical axis orientation of each layer as a possible

fitting parameter makes this technique capable to give information also on director profile of liquid crystals through cell thickness.

The method was first tested on known structures: an isotropic semi-infinite sample, simply a glass prism, and an isotropic layered structure, which was the same prism covered by an ITO layer. Then the method was finally used to characterise an anisotropic multilayered structure consisting of a 5CB liquid crystal cell.

In the isotropic case we got results in good agreement both with values computed by a commercial software and values of refractive indices reported in the prism glass data sheet. Birefringence dependence versus wavelength measured for the 5CB cell showed an accuracy within 1% when compared with data reported in the literature.

## EXPERIMENTAL SETUP

A Phase Modulated Ellipsometer by ISA Jobin-Yvon used in our experiments is schematically sketched in Figure 1, as reported in the instrument handbook. An argon lamp, used as light source, feeds an optical fiber then light goes through a polarizer. After a collimation optical system the light beam impinges on the sample surface, being then reflected towards a modulator and an analyser. Hence the optical signal goes through an optical fiber connected to a monochromator, which has two outputs: a photomultiplier for visible light spectrum and a CCD for near infrared spectrum.

Detected electric field, as a function of all optical and geometrical parameters of the system, can be carried out by using Jones calculus [11] as follows:

$$\mathbf{E}_{\text{out}} = T[\mathbf{A} \cdot \mathbf{R}(\beta - \mu) \cdot \mathbf{M} \cdot \mathbf{R}(\mu) \cdot \mathbf{S} \cdot \mathbf{R}(-\alpha) \cdot \mathbf{P}] \mathbf{E}_i \quad (1)$$

where  $\mathbf{P}$  and  $\mathbf{A}$  are the Jones matrices of the polarizer and analyzer respectively,  $\mathbf{R}(\ )$  are the rotation matrices,  $\alpha$ ,  $\beta$ ,  $\mu$  are the rotating angles of polarizer, analyzer and modulator, respectively in the lab reference system.  $\mathbf{E}_i = \mathbf{R}(\alpha) \mathbf{E}_{\text{in}}$ , where  $\mathbf{E}_{\text{in}}$  is the input electric field.  $T$  is a normalization factor.

$\mathbf{S} = \begin{pmatrix} s_{pp} & s_{ps} \\ s_{sp} & s_{ss} \end{pmatrix}$  is the sample reflection matrix, which is diagonal for an isotropic sample and non-diagonal for an anisotropic sample, where s stands for the s-polarized (TE) radiation, along the y axis, and p stands for the p-polarized (TM), in the xz plane;  $\mathbf{M} = \begin{pmatrix} e^{j\delta} & 0 \\ 0 & 1 \end{pmatrix}$  is the modulator Jones matrix where  $\delta(t) = \delta_0 + A \sin \omega t$ .

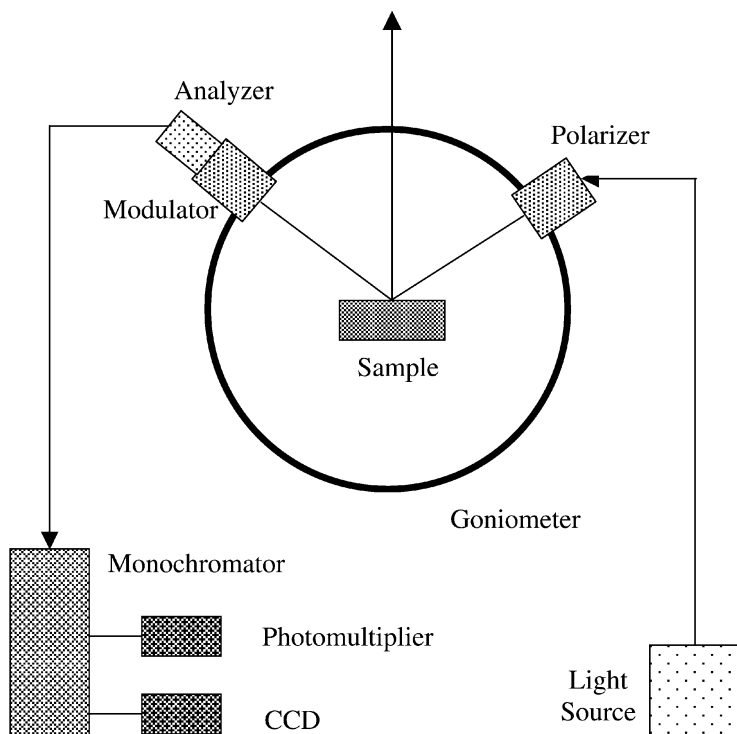


FIGURE 1. Schematic of the Jobin-Yvon UVISEL 460 phase modulated ellipsometer.

The intensities of the detected signal contain the continuous, sinusoidal and cosinusoidal components of the modulated signal:

$$I(t) \propto \mathbf{E}_{\text{out}} \mathbf{E}_{\text{out}}^* = I[I_0 + I_s \sin \delta(t) + I_c \cos \delta(t)] \quad (2)$$

It is possible to get the three components of the right-hand side of (2) as a function of Jones matrix elements by using (1) in the left-hand side of (2).

A set of independent equations in terms of amplitude and phase of reflection coefficients,  $s_{ij} = \rho_{ij} \exp(j\varphi_{ij})$  is obtained by calculating intensity expressions for a few couples of angles for the analyzer and the polarizer, setting a fixed difference between analyzer and modulator orientation equal to  $45^\circ$ .

For polarizer orientation equal to  $0^\circ$  and modulator axis equal to  $-45^\circ$  we obtain:

$$\begin{aligned} I_0 &= \frac{|T|^2}{2} (\rho_{pp}^2 + \rho_{sp}^2) \\ I_c &= \frac{|T|^2}{2} (\rho_{pp}^2 - \rho_{sp}^2) \\ I_s &= -|T|^2 \rho_{sp} \rho_{pp} \sin(\varphi_{pp} - \varphi_{sp}) \end{aligned} \quad (3)$$

For polarizer at  $90^\circ$  and modulator at  $45^\circ$ :

$$\begin{aligned} I_0 &= \frac{|T|^2}{2} (\rho_{ps}^2 + \rho_{ss}^2) \\ I_c &= \frac{|T|^2}{2} (\rho_{ss}^2 - \rho_{ps}^2) \\ I_s &= |T|^2 \rho_{ss} \rho_{ps} \sin(\varphi_{ss} - \varphi_{ps}) \end{aligned} \quad (4)$$

For polarizer at  $45^\circ$  and modulator at  $0^\circ$ :

$$\begin{aligned}
I_0 &= \frac{|T|^2}{4} [\rho_{pp}^2 + \rho_{sp}^2 + \rho_{ps}^2 + \rho_{ss}^2 + 2\rho_{pp}\rho_{ps} \cos(\varphi_{pp} - \varphi_{ps}) + \\
&\quad + 2\rho_{sp}\rho_{ss} \cos(\varphi_{sp} - \varphi_{ss})] \\
I_c &= \frac{|T|^2}{2} [\rho_{pp}\rho_{sp} \cos(\varphi_{sp} - \varphi_{pp}) + \rho_{sp}\rho_{ps} \cos(\varphi_{sp} - \varphi_{ps}) + \\
&\quad + \rho_{pp}\rho_{ss} \cos(\varphi_{pp} - \varphi_{ss}) + \rho_{ss}\rho_{ps} \cos(\varphi_{ps} - \varphi_{ss})] \\
I_s &= -\frac{|T|^2}{2} [\rho_{pp}\rho_{sp} \sin(\varphi_{pp} - \varphi_{sp}) + \rho_{sp}\rho_{ps} \sin(\varphi_{ps} - \varphi_{sp}) + \\
&\quad + \rho_{pp}\rho_{ss} \sin(\varphi_{pp} - \varphi_{ss}) + \rho_{ss}\rho_{ps} \sin(\varphi_{ps} - \varphi_{ss})]
\end{aligned} \tag{5}$$

Equations (3)-(5) were employed to extract information about off-diagonal elements of the refraction matrix  $\mathbf{S}$ , tied to the anisotropic properties of the material sample.

#### APPLICATION OF PME TO ANISOTROPIC LAYERED STRUCTURE

The direct inversion of ellipsometric measurements can be obtained only in some special cases of single interface: either between semi-infinite isotropic materials or between isotropic-anisotropic with specific orientation of the optical axes.

Our purpose is to characterise an anisotropic multilayered structure schematically drawn in Figure 2, where several anisotropic layers, with any optical axis orientation, are sandwiched between isotropic semi-infinite ambient and substrate, like in a liquid crystal cell whose thickness has been divided into several layers. For such a structure it is impossible to derive optical properties of each layer simply starting from ellipsometer measurements or from reflection matrix. On the contrary it is always possible to calculate the reflection coefficients, starting from the knowledge of the structure and its optical properties by using Berreman's formalism [12]. According to it, each layer is then represented by a 6x6 matrix  $\mathbf{B}_i$  whose elements consist of

the dielectric tensor  $\underline{\underline{\epsilon}}$ , the magnetic tensor  $\underline{\underline{\mu}}$  and two optical activity tensors  $\underline{\underline{\rho}}$  and  $\underline{\underline{\rho'}}$ .

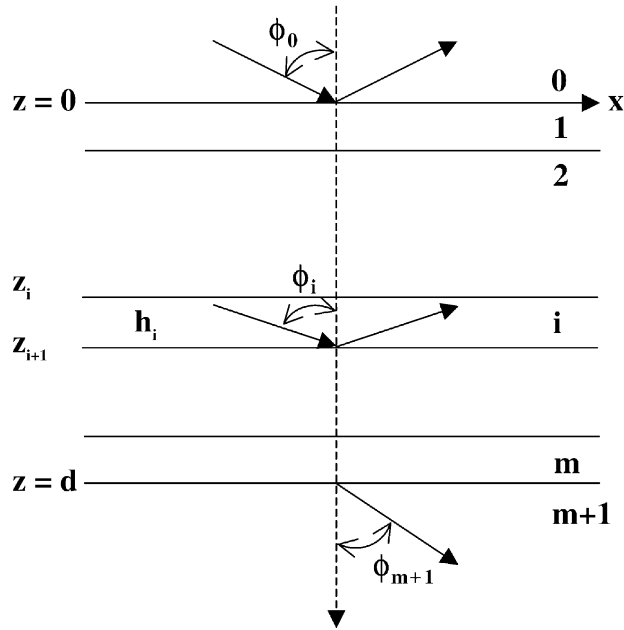


FIGURE 2. Sketch of a multilayered structure with definition of incidence angles at each layer interface. The layer  $m+1$  is the substrate.

Considering planar monochromatic waves travelling along  $z$  direction, the four Maxwell's equations can be written in a compact form as:

$$\frac{\partial}{\partial z} \Psi = \frac{i\omega}{c} \Delta \Psi \quad (6)$$



where:

$$\Psi = \begin{bmatrix} E_x \\ H_y \\ E_y \\ H_x \end{bmatrix} \text{ and } \Delta = \begin{bmatrix} \Delta_{11} & \Delta_{12} & \Delta_{13} & \Delta_{14} \\ \Delta_{21} & \Delta_{22} & \Delta_{23} & \Delta_{24} \\ \Delta_{31} & \Delta_{32} & \Delta_{33} & \Delta_{34} \\ \Delta_{41} & \Delta_{42} & \Delta_{43} & \Delta_{44} \end{bmatrix} \quad (7)$$

with  $\Delta$  directly linked with matrix  $\mathbf{B}_{(i)}$ .

Considering light propagation through a layer between  $z_i$  and  $z_{i+1} = z_i + h_i$ ,  $h_i$  being the thickness of the  $i^{\text{th}}$  layer and integrating Maxwell's equation (6) we obtain:

$$\Psi(z_{i+1}) = \mathbf{L}(h_i) \Psi(z_i) \quad (8)$$

where:

$$\mathbf{L}(h_i) = \exp\left(i \frac{\omega h_i}{c} \Delta\right) = \mathbf{I} + i \frac{\omega h_i}{c} \Delta - \left(\frac{\omega h_i}{c}\right)^2 \frac{1}{2!} \Delta \cdot \Delta + \dots \quad (9)$$

Now solving (6) from  $z = 0$  to  $z = d$  with boundary conditions for which there is an incident and a reflected wave at  $z = 0$  and only a transmitted wave at  $z = d$ :

$$\Psi_i = \begin{bmatrix} E_x \\ r_x E_x \\ E_y \\ r_y E_y \end{bmatrix} \text{ with } \begin{matrix} r_x = n_0 / \cos \varphi_0 \\ r_y = n_0 \cos \varphi_0 \end{matrix} \quad (10)$$

$$\Psi_r = \begin{bmatrix} R_x \\ -r_x R_x \\ R_y \\ -r_y R_y \end{bmatrix} \quad (11)$$

$$\Psi_t = \begin{bmatrix} T_x \\ -r'_x T_x \\ T_y \\ -r'_y T_y \end{bmatrix} \quad \text{with} \quad \begin{aligned} r'_x &= n_{m+1} / \cos \varphi_{m+1} \\ r'_y &= n_{m+1} \cos \varphi_{m+1} \end{aligned} \quad (12)$$

where  $R_x$  and  $T_x$  are the amplitude of reflected and transmitted fields,  $n_0$  and  $n_{m+1}$  are ambient and substrate refractive indices respectively;  $\varphi_0$  is the incident ray angle measured respect to the normal to the surface ( $z$  axis) and  $\varphi_{m+1}$  is the angle of the transmitted ray in the substrate (see Fig. 2).

From the Snell's law:  $\varphi_{m+1} = \sin^{-1} \left[ \frac{n_0}{n_{m+1}} \sin \varphi_0 \right]$ . For the whole

structure:  $\Psi(z+d) = \mathbf{L}_{\text{tot}}(d) \Psi(z)$ , where  $\mathbf{L}_{\text{tot}}(d) = \prod_{i=1}^n \mathbf{L}(h_i)$ . In this

way the reflection coefficients of Jones' matrix can be obtained for the whole structure, as:

$$s_{pp} = \frac{R_x}{E_x}; s_{ps} = \frac{R_y}{E_x}; s_{sp} = \frac{R_x}{E_y}; s_{ss} = \frac{R_y}{E_y} \quad (13)$$

Berremen's formalism gives the possibility to calculate directly the reflection coefficients also for a multilayered complex structure. Six independent parameters, real and imaginary part of  $s_{ij}$  normalised respect to  $s_{pp}$ , are then used in Eq. (3)-(5) to calculate normalised intensities  $I_c/I_0$  and  $I_s/I_0$  providing six independent equations from the three ellipsometric configurations.

A fitting algorithm was developed based on the minimization of an error function  $\chi^2$  between calculated normalized intensities and those ones measured by the ellipsometer:

$$\chi^2 = \sum_{i=1}^N \left[ \left( \frac{I_C^{\text{mis}}}{I_0^{\text{mis}}} - \frac{I_C^{\text{cal}}}{I_0^{\text{cal}}} \right)_i^2 + \left( \frac{I_S^{\text{mis}}}{I_0^{\text{mis}}} - \frac{I_S^{\text{cal}}}{I_0^{\text{cal}}} \right)_i^2 \right] \quad (14)$$

where  $N = 3$  is the maximum number of independent configurations of the ellipsometer.

In general each layer is characterised by:

- complex dielectric constants  $\epsilon_1$ ,  $\epsilon_2$  and  $\epsilon_3$  in the principal reference system;
- Euler's angles  $\phi$ ,  $\psi$ , and  $\theta$  which define the orientation of principal reference system respect to the laboratory reference system;
- layer thickness  $d$ .

The number of unknowns for each layer are as follows: three unknowns, real and imaginary part of  $\epsilon_1 = \epsilon_2 = \epsilon_3$  and  $d$  if the layer is isotropic; seven unknowns, real and imaginary part of  $\epsilon_1 = \epsilon_2 \neq \epsilon_3$ ,  $d$  and two Euler's angles if the unknown layer is uniaxial; ten unknowns real and imaginary part of  $\epsilon_1 \neq \epsilon_2 \neq \epsilon_3$ ,  $d$  and all of three Euler's angles, if the layer is biaxial.

## MEASUREMENTS AND CONCLUSIONS

Refractive indices of few samples were measured by using the proposed extension of PME technique for a wavelength spectrum ranging from 300 nm to 1600 nm.

Figure 3 shows the plot of refractive index dispersion curve of a Corning FBS E78-38 glass prism. Triangle dots refer to values computed by using our software code, square dots represent values obtained by using the version 4.3 of the ellipsometer commercial software "Elli43" and finally continuous line is the dispersion curve according to Sellmeier equation as reported by the prism glass data sheet. The plot shows that our software and the commercial one give the same values and accuracy respect to Sellmeier's equation.

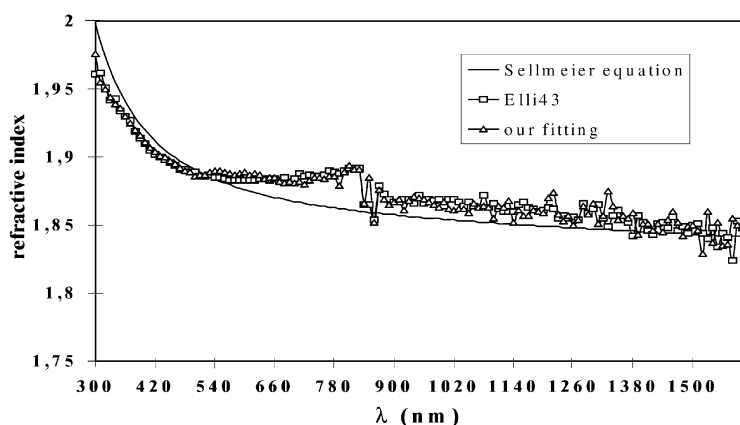


FIGURE 3. Refractive index dispersion of Corning FBS E78-38 glass prism: comparison among values obtained by PME extension based fitting code (triangles), ellipsometer software (squares) and Sellmeier equation (solid line).

The same prism with an ITO layer of known thickness was also characterised. Plots of ITO real and imaginary part of the refractive index obtained by both “Elli43” and our fitting code are reported in Figure 4.

There is good agreement between the two plots of the real part of the ITO refractive index over the visible range of the spectrum. A decrease of the solid line plot starting at the wavelength about 900 nm is due to a decrease of light intensity.

The difference between solid and dotted lines in Figure 4 increases with wavelength because Elli43 software fits the parameter of a given dispersion law over the entire spectrum. Moreover values given by ellipsometer software are locally independent by detected light. On the contrary our fitting is performed at each wavelength and is directly dependent on signal to noise value of detected light.

Finally a cell filled with liquid crystal 5CB with known thickness, about 10  $\mu\text{m}$  and director orientation known was characterised by using

the phase modulated ellipsometer. In these calculations liquid crystal thickness and director orientation are considered as fixed parameters.

Figure 5 shows the dispersion curves of both extraordinary and ordinary refractive index computed by using our data fitting analysis. It also includes dispersion curves obtained by using refractometric technique reported in [13] for a similar liquid crystal cell.

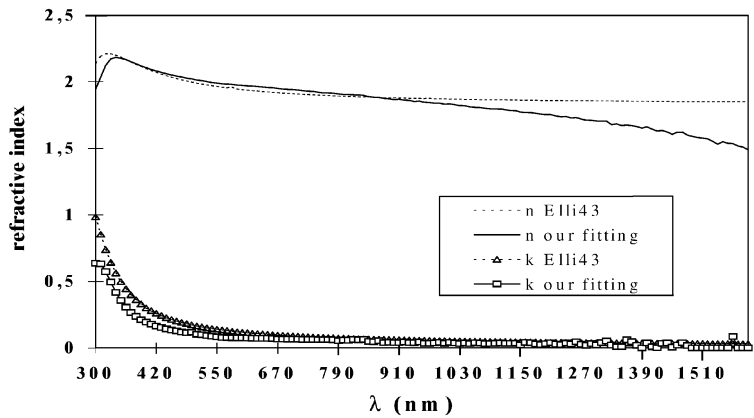


FIGURE 4. Dispersion of real part ( $n$ ) and imaginary part ( $k$ ) of refractive index ITO deposited on Corning FBS E78-38 glass prism: comparison among values obtained by ellipsometer software and PME extension based fitting code.

The plots obtained with the two techniques show very similar behaviour with difference in the worst case of about 4%, due to the different temperature at which the measurements were performed.

Our measurements were performed at about 22°C, while in reference [13] measurements were performed at 25.1°C. As expected the values of indices and birefringence decrease as temperature

increases. In addition, it is possible to check that for a specific wavelength (He-Ne, 0.6328  $\mu\text{m}$ ) our measurement at 22  $^{\circ}\text{C}$  is consistent with the one obtained in ref. [2] at 21  $^{\circ}\text{C}$  using TIR.

These preliminary measurements have not been optimised in terms of substrate and ambient dielectric function, explaining partly the discrepancy between the values shown in Figure 5. Furthermore plots from PME measurements also show a decrease of birefringence as wavelength increases, as expected.

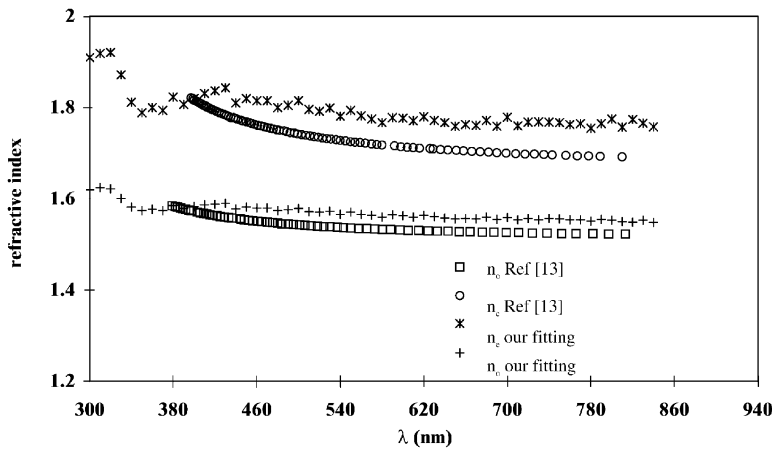


FIGURE 5. Dispersion of ordinary,  $n_o$ , and extraordinary,  $n_e$ , refractive index of liquid crystal 5CB: comparison between values obtained by extension PME code and values obtained in ref. [13].

In conclusions we derived a software code to process measurements performed by PME on anisotropic layered samples. In particular each anisotropic layer can have any arbitrary optical axis orientation, hence in principle the technique can be also used to study liquid crystal director profile by considering the cell thickness divided into several layers and by supposing a particular director profile law. We carried out some test measurements which proof that our software

code can be used to measure refractive index of liquid crystals confined in planar cells. The accuracy of this measurement technique is about 1% basically due to the mechanical parts, especially the sample holder and the goniometer of the ellipsometer. Nevertheless it is a fast technique to obtain readily dispersion of refractive indices over a broad spectrum from visible to near-infrared of paramount interest for most photonic applications.

### Acknowledgements

This work has been accomplished in the frame of the EU funded BRITE Network "LC-PHOTONET". The Laboratoire de Physico-Chimie des Interfaces et Applications participates to the Centre d'Etudes et de Recherches sur les Lasers et Applications, supported by the Ministère chargé de la Recherche, the "région Nord/Pas de Calais" and the "Fonds Européen de Développement Economique des Région". Finally the authors wish to thank Rita Asquini for critical reading this manuscript.

### References

- [1] M. Brunet Germain, CRAS, **271**, 1075, (1970).
- [2] M. Warengem, M. Ismaili, D. Hector, J. Phys. III France, **5**, 765, (1992).
- [3] M. Warengem, G. Joly, Mol. Cryst. Liq. Cryst., **207**, 205, (1991).
- [4] F. Yang, J. R. Sambles, J. Opt. Soc. Am. B, **10**, 858 (1993).
- [5] F. Simoni, F. Bloisi, L. Vicari, M. Warengem, M. Ismaili, D. Hector, Eur. Phys. Lett., **21**, 189 (1993).
- [6] S. Elston, R. Sambles, Appl. Phys. Lett., **55**, 1621 (1989).
- [7] S. Okutano, M. Rimura, T. Akahane, H. Toriumi, T. Tadokoro, K. Akao, Mol. Cryst. Liq. Crystal, **329**, 269 (1999).
- [8] G. E. Jellison, Jr. F. A. Modine, L. A. Boatner, Optics Letters, **22**, 1808 (1997).
- [9] J. Lekner, J. Opt. Soc. Am. A, **14**, 1359 (1997).

- [10] M. Schubert, B. Rheinländer, J. A. Woollam, B. Johs, C. M. Herzinger, J. Opt. Soc. Am. A, **13**, 875 (1996).
- [11] R.C Jones, J. Opt. Soc. Am., **31**, 488 (1944).
- [12] D. W. Berreman, J. Opt. Soc. Am. A, **62**, 502 (1972).
- [13] S. T. Wu, C. S. Wu, M. Warengem, M. Ismaili, Optical Engineering, **32**, 1775 (1993).